Nuclear Instruments and Methods in Physics Research B 299 (2013) 24–28

Contents lists available at SciVerse ScienceDirect

Nuclear Instruments and Methods in Physics Research B

journal homepage: www.elsevier.com/locate/nimb

Ion channeling in $CuInSe_2$ single crystals

Michael V. Yakushev *, Vladimir A. Volkov, Ilya I. Ogorodnikov, Vladimir U. Ivanov

Urals Federal University, 620002 Ekaterinburg, Russia

ARTICLE INFO

Article history:
Received 3 October 2012
Received in revised form 24 January 2013
Available online 8 February 2013

Keywords:
$CuInSe_2$
Ion channeling
Defects

ABSTRACT

$CuInSe_2$ single crystals are studied by the Rutherford Backscattering of 2 MeV helium ions involving axial channeling along the ⟨2 2 1⟩ direction of the chalcopyrite lattice. Experimental values of the critical angle and normalized minimum yield are measured and compared with theory. The concentration of point defects separately in the Cu, In, and Se sublattices, determined from the comparison of experimental and theoretical minimum yields, are estimated as 4.7×10^{20}, 1.0×10^{20}, and 5.7×10^{20} cm^{-3}, respectively.

1. Introduction

$CuInSe_2$-based solar cells are leading (in terms of conversion efficiency and stability) thin film photovoltaic (PV) devices. Their record efficiency on a laboratory scale is exceeding 20% [1]. However the gap between this value and the theoretical limit of efficiency (about 30% [2] for a single junction solar cell) is very significant suggesting a lack of knowledge on the basic physical properties of $CuInSe_2$. Very little experimental evidence can be found in the literature on intrinsic structural defects although such defects are used for doping $CuInSe_2$ [3] to control the electric properties consequently influencing the performance of the $CuInSe_2$-based solar cells.

Concentrations of defects in $CuInSe_2$ have mostly been estimated using Hall effect [3], optical absorption [4,5], deep level transient spectroscopy [6], neutron diffraction [7] and positron annihilation [8]. However each of these techniques is sensitive to particular defect types corresponding to the physical effect used for the characterisation.

One of the experimental methods, which can provide reliable information on the total concentration of structural defects in single crystals of semiconductors is Rutherford Backscattering (RBS) combined with ion channeling effect (RBS-C) [9]. Aligning a beam of high energy positively charged ions along a low index crystal axis results in a significant reduction of the backscattered yield which become very sensitive to imperfections of the lattice and in particular to atoms shifted from their lattice positions to interstitial sites blocking the channels, space between the axial rows of atoms in the lattice. However this technique requires high-energy ion accelerators which are available in quite a limited number of the world research centres. Also successful application of RBS-C requires high structural quality single crystals which are difficult to grow due to complicated phase diagram of $CuInSe_2$. Therefore very few publications reporting the use of RBS-C for studies of $CuInSe_2$ and related compounds can be found in the literature. These publications concentrate mostly on relative changes in the aligned spectra before and after various modifications of the near surface layers of $CuInSe_2$ [10–12]. Only one report [13] attempts to compare minimum yields χ_{min} in the aligned spectra of $CuInSe_2$, a basic experimental parameter of ion channeling, with theoretical values and estimate defect concentrations in this material. However in this report only the indium sublattice was analysed whereas the determined defect concentrations were attributed to the whole lattice. No angular yield dependencies of RBS yield in $CuInSe_2$ have been published as yet.

In this paper we present results of experiments on the channeling of He ions in high structural quality $CuInSe_2$ single crystals. Critical angle of dechanneling $\psi_{1/2}$ and normalised minimum yields χ_{min}, determined separately for the Cu, In, and Se sublattices, were compared with theoretical values. Defect concentrations were estimated separately for each sublattice.

2. Materials and methods

Single crystalline ingots of $CuInSe_2$ were grown using the vertical Bridgman technique [14]. Samples of about 2 mm thick with dimensions of 7×7 mm^2 were cut from middle parts of the ingots perpendicular to the direction of growth by a diamond wire saw. Surfaces of the samples were prepared for RBS-C experiments by polishing with different grades of diamond pastes from 5 to 1 μm, etching in 5% bromine–methanol solution and annealing at 300 °C. Details of this procedure are described in Ref. [10]. X-ray diffraction (XRD) measurements show the presence of only

* Corresponding author.
E-mail address: michael.yakushev@strath.ac.uk (M.V. Yakushev).

0168-583X/$ - see front matter © 2013 Elsevier B.V. All rights reserved.
http://dx.doi.org/10.1016/j.nimb.2013.01.039

chalcopyrite phase. The chalcopyrite structure of $CuInSe_2$ can be derived from the cubic sphalerite one of ZnSe by an ordered replacement of Zn with alternating Cu and In. The difference in the Cu–Se and In–Se bonding results in a small tetragonal distortion $\tau = 1 - c_0/2a_0$ of the lattice [15], where $a_0 = 0.5783$ and $c_0 = 1.1620$ nm are the lattice parameters along and perpendicular to the tetragonal direction, respectively, for the analysed samples. In the characterised samples τ was measured to be of about −0.5%. Because of the small value of this distortion we assumed the lattice to be diamond-like where $c_0 \approx 2a_0$.

Using Energy Dispersive X-ray analysis (EDX) the elemental composition of the samples was found to be close to the ideal stoichiometry Cu:24.2, In:25.9, and Se:49.9 at.%. Electron channelling (Kikuchi) patterns (ECP) were obtained from various points across the surfaces prepared for RBS-C experiments. The similarity of such patterns was taken as evidence that the samples are single crystals. In all the samples the ⟨2 2 1⟩ crystallographic direction of the chalcopyrite structure, corresponding to the ⟨1 1 1⟩ direction in diamond structure, was found to be within 5° from the normal to the surface.

The RBS-C measurements were carried out using a beam of 2 MeV He ions from a Van de Graaff accelerator incident to the surface. A scattering angle of 168° has been employed. The yield of backscattered He ions was detected by a surface barrier solid state detector with an energy resolution of 25 keV. The analyser channel number x in our RBS spectra is proportional to an energy E of the backscattered ions as $E = \delta x$, where $\delta = 5$ keV corresponding to one channel of the analyser. The total number of incident ions has been evaluated by measuring the charge delivered to the samples. For the RBS spectra charges of either 20 or 40 μC have been collected. The channeling mode experiments have been carried out along the ⟨2 2 1⟩ axis using a goniometer with two perpendicular axes of rotation (φ and θ angles) with reproducibility of 0.02°. The random spectra were collected directing the ion beam 5° away from the ⟨2 2 1⟩ axis while slowly tilting the samples about this axis to avoid channeling effect from axes and planes.

3. Results

3.1. Aligned and random spectra

Typical 40 μC RBS random and ⟨2 2 1⟩ axis aligned spectra are shown in Fig. 1. RBS spectra from ternary compounds can be considered as the sum of three RBS yields corresponding to the three elements constituting the compound. Each yield is shifted on the energy scale according to the element mass. The random spectrum

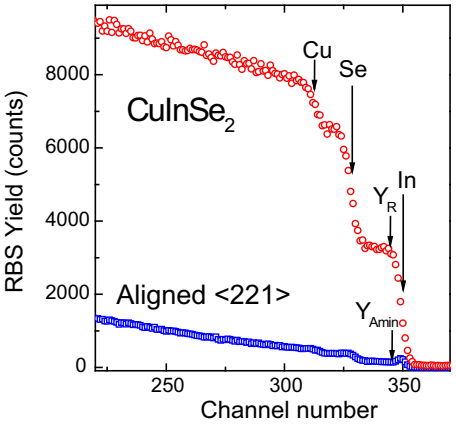

Fig. 1. RBS aligned (□), for the He ion beam oriented along the ⟨2 2 1⟩ direction, and random (○) spectra in $CuInSe_2$ single crystals.

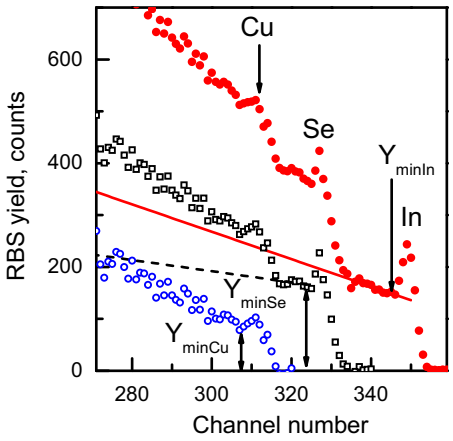

Fig. 2. RBS ⟨2 2 1⟩ aligned spectrum (●), Se (□), and Cu related aligned RBS yields (○). The regression lines, extrapolating flat parts of the indium and selenium aligned yields, are solid and dash lines, respectively.

in Fig. 1 reveals three distinct shoulders associated with the RBS yields from In, Se and Cu. The edges of the shoulders have shapes of integrated Gaussians due to limited resolution of the measurements. The channel numbers corresponding to the three atomic species on the surface are shown by the arrows. Directing the He ion beam along the ⟨2 2 1⟩ axis causes a dramatic reduction in the backscattering due to the axial channeling effect.

The aligned spectrum is shown in Fig. 2 using a reduced scale. The two well resolved surface peaks in this spectrum, associated with direct backscattering from In and Se atoms on the surface, can clearly be seen due to the large RBS cross sections of these elements whereas the Cu-related peak is less distinct due to a smaller RBS cross section of Cu. The gradual increase of the RBS dechanneling background with depth is caused by thermal vibrations of the lattice atoms and structural defects causing a gradual increase of the mean transverse energy of the channeling particles which increases the probability of dechanneling and large angle scattering. The high-energy edge of the aligned spectrum corresponds to scattering from the near surface layer. Helium ions lose their energy as they move through the crystal so the aligned spectrum beyond the surface peak represents a progressively increasing depth. The minimum yield and slope of the aligned spectrum are used as parameters of the structural quality: the smaller the minimum yield and the slope the higher the structural lattice quality.

3.2. Angular dependence of aligned yield

The angular dependence of the RBS spectra has been measured by tilting the ⟨2 2 1⟩ axis of the crystal through the beam direction. The normalised yield $\chi(\varphi)$ has been calculated as the sum of the yields in 7 channels right before the indium surface peak in the RBS spectra at each angle divided by the sum of the yields in the random spectrum in the 7 corresponding channels. This angular dependence is shown in Fig. 3.

The critical angle $\psi_{1/2} = 0.80° \pm 0.02°$, determined as the half width at the midway between χ_{min} and unity, corresponding to the normalised random yield, is related to the indium sublattice of $CuInSe_2$. Critical angles for axial channeling can be estimated by the characteristic angle ψ_1 of the Lindhard's theory [16] as $\psi_{1/2} = \alpha\psi_1$ where the value of α can be between 0.8 and 1.2 depending on the vibrational amplitudes of the lattice atoms [9]. The Lindhard's theory has been adopted by Picraux et al. [17] for the case of channeling in lattices with diamond like structures of multinary compounds. At the condition $\psi_1 \leqslant a/d$, where a is the Thomas–Fermi screening distance and d is the average lattice spacing along the axis, ψ_1 can be calculated [16] as:

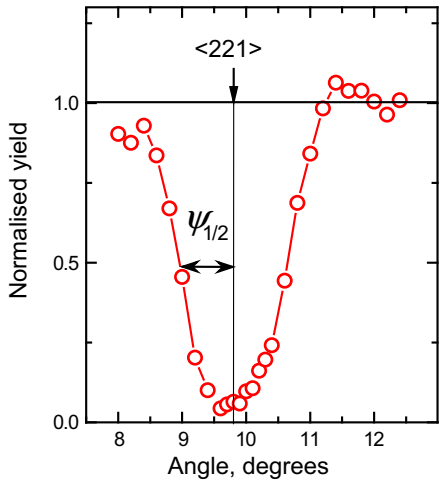

Fig. 3. The angular dependence of the normalised RBS yield from the In sublattice about the ⟨221⟩ axis.

$$\psi_1 = \sqrt{2Z_1Z_2e^2/Ed}, \quad (1)$$

where Z_1 are Z_2 are the atomic numbers of the projectile and average atomic number of the target atoms, respectively, e is the charge of electron, and E is projectile energy. Traversing $CuInSe_2$ along ⟨221⟩ rows of atoms, containing three types of atomic species, channeling ions are influenced by the average potential of the rows. For such a potential average atomic spacing d and average atomic number Z_2 can be used.

The average atomic spacing along the ⟨221⟩ direction was calculated as $d = a_0\sqrt{3}/2$ [17] making $d = 0.5002$ nm. The string of atoms along the ⟨221⟩ axis contains all the three atomic species Cu, In and Se in the proportion [Cu]:[In]:[Se] = 1:1:2 therefore the average atomic number can be calculated as $Z_2 = (Z_{Cu} + Z_{In} + 2\text{-}Z_{Se})/4$. Thus for the ⟨221⟩ axis $\psi_1 = 0.83^o$ (0.014 rad). The Thomas–Fermi screening distance was calculated assuming the d and Z_2 averaged along ⟨221⟩:

$$a = 0.8853 \cdot a_B/\sqrt{Z_1^{2/3} + Z_2^{2/3}}, \quad (2)$$

where a_B is the Bohr radius. The ratio $a/d = 0.026$ rad is greater than ψ_1 confirming the validity of expression (1).

The calculated value of ψ_1 is very close to the experimental $\psi_{1/2}$ making the ratio $\psi_{1/2}/\psi_1 = \alpha = 0.965$ very close to unity which is very similar to $\alpha = 1.00$ in GaAs and Ge measured using 1.9 MeV He ions whereas in GaP $\psi_{1/2}$, measured from the RBS yield of heavier Ga, is noticeably greater than ψ_1 making $\alpha = 1.17$ in GaP [17].

3.3. Minimum yield

The normalised minimum yield χ_{min} is calculated as $\chi_{min} = Y_{Amin}/Y_R$, the ratio of the minimum spectral yield in aligned spectrum Y_{Amin} and the random spectrum yield Y_R at the same channel number as shown in Figs. 1 and 2. Random and ⟨221⟩ aligned spectra were measured in a number of $CuInSe_2$ samples. The value of χ_{min} in these samples varied from 3.8% to 14% depending on the quality of the crystal lattice. The $CuInSe_2$ crystals of the highest available structural quality have been chosen to estimate concentrations of structural defect in the lattice. Three aligned spectra, two for 20 and one for 40 μC, measured at three different points across the surface of this sample are shown in Fig. 4. Their intensities are normalised according to their charges for comparison. It can be seen that the structural quality of the lattice in these three points is quite similar although some scatter is present. The two

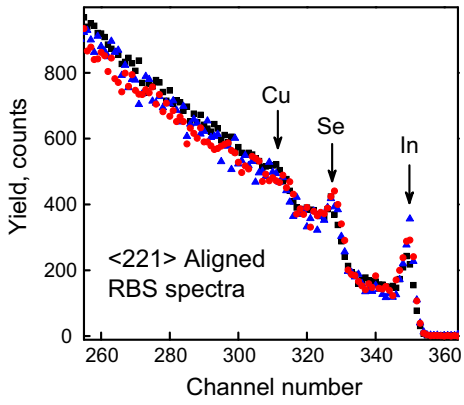

Fig. 4. A comparison of the aligned spectra measured at different points of the surface of the same $CuInSe_2$ crystal.

Table 1
Normalised values of the experimental RBS minimum yields $\chi_{min\text{-}ex}$ averaged over the three aligned spectra and their statistical errors of the mean reflecting the precisions, mean squared values of thermal vibration amplitudes u, theoretical RBS minimum yields $\chi_{min\text{-}th}$, and estimates of the defect concentrations for the Cu, In, and Se sublattices (absolute values N_d and normalised by the atomic densities of the elements n_d).

Sublattice	Cu	In	Se
$\chi_{min\text{-}ex}$, %	6.4 ± 0.8	4.3 ± 0.2	5.6 ± 0.2
u, nm	0.0134	0.0186	0.0121
$\chi_{min\text{-}th}$, %	1.8	3.4	2.9
N_d 10^{20}, cm^{-3}	4.9 ± 0.9	1.0 ± 0.3	5.7 ± 0.4
n_d, %	4.7 ± 0.8	0.9 ± 0.3	2.8 ± 0.2

20 μC spectra demonstrate a greater scatter than the 40 μC one. To calculate Y_{Amin} the sum of the yields in three consecutive channels in each aligned spectrum just before the indium surface peak were divided by the sum of the three corresponding channel yields in the random spectra Y_R. An average value of $\chi_{min\text{-}ex} = 4.3\% \pm 0.2\%$, where 0.2% is the statistical error of the mean [18] reflecting the precision for the three measurements. In monatomic crystals the minimum yield χ_{min} represents structural quality of the whole lattice whereas in multinary compounds χ_{min} with significantly different masses of the constituent elements is related to the RBS yield from the heaviest element and represents structural quality of the heaviest element sublattice.

In $CuInSe_2$, the high energy part of the RBS spectra, channels from 330 to 355, are associated with In. The yield from the next heaviest element, Se, is shifted by about 21 channels towards lower energies overlapping the yield from In before the 330 channel. The yield from the lightest element, Cu, is shifted towards lower energies by further 15 channels overlapping both yields from In and Se. Therefore both Y_{Amin} and Y_R, shown in Fig. 1, as well as their ratio χ_{min} are associated with just the indium sublattice. Therefore $\chi_{min\text{-}ex} = 4.3\%$, shown in Table 1, is associated with the In sublattice.

To determine Y_{minSe}, associated with just selenium sublattice, the indium RBS yield has to be subtracted from the total aligned spectrum. The flat and monotonous high-energy part of RBS aligned spectra before the corresponding surface peak can be approximated by straight line. Such linearity, up to the surface peaks in the aligned spectra, can clearly be seen in Figs. 1, 2 and 4. The flat and monotonous shape of the RBS random yield between the edge corresponding to the surface for each element and the beginning of a lighter element shoulder suggests a depth homogeneous elemental composition of $CuInSe_2$ in the near surface layer. The flat and monotonous shape of the aligned spectrum between the surface peaks suggests a depth homogeneous

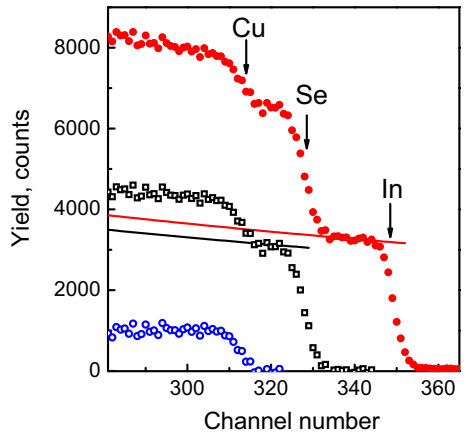

Fig. 5. RBS random spectrum taken for $CuInSe_2$ single crystals (●), Se and Cu related random RBS yield (□), Cu related random RBS yield (○), the regression lines, extrapolating the indium and selenium random yields, are solid and dash lines, respectively.

defect concentration within the layer corresponding to the energy range of the spectrum. The indium related part of the aligned spectrum before the In surface peak was approximated by a straight regression line fitted to the experimental points of the aligned spectrum between the In and Se surface peaks as shown in Fig. 2. To estimate Y_{minSe} for the Se sublattice this line, extrapolating the indium aligned yield under the selenium one, has been subtracted from the aligned spectrum. The Se aligned yield after such a subtraction is shown in Fig. 2.

To estimate Y_R in the Se sublattice the experimental points of the random spectrum, corresponding to flat In shoulder was fitted with the function $A/(E_0+E)^2$, where E_0 is the energy of incident ions, E is the energy of a detected ion, that produces counts in channel x and A fitting parameter [19]. Fig. 5 shows the fitted curves as well as the Se random spectrum after the subtraction. A normalised minimum yield of $\chi_{minSe} = (5.6 \pm 0.2)\%$ for the Se sublattice, calculated as an average value for the three aligned spectra, is shown in Table 1. Where 0.2% is the prescision for the three measurements.

The accuracy of the Se aligned yield is determined by the error of the intercept and slope of the straight regression line $y = y_0 + kx$, where y is an approximation of the experimental yield Y in channel x, y_0 intercept and k slope, best fitted into the experimental data. An error of the normalised Se minimum yield of ±9.3% is quite significant. Because it exceeds the normalised minimum yield for Se we can estimate only the upper possible limit of χ_{minSe} to be about 15%. It includes both the error of the extrapolation by the regression line at the channels corresponding to Y_{minSe} in the Se aligned yield and the error of Y_R in the Se random yield, extrapolated by $A/(E_0+E)^2$, at the corresponding channels. However the error of the mean, precision of χ_{minSe} for the three aligned spectra is ±0.2% as shown in Table 1.

A similar procedure has been used to decompose Se and Cu related aligned yields by subtracting the Se related one, approximated by a regression line fitted to the experimental points of the Se aligned spectra, as shown in Figs. 2 and 4. The random spectrum, corresponding to the flat Se shoulder was also fitted with the function $A/(E_0+E)^2$ as shown in Fig. 5.

A normalised minimum yield of $\chi_{minCu} = 6.4\%$ for the Cu sublattice, calculated as an average value for the three aligned spectra, is shown in Table 1.

The accuracy of the Cu aligned yield is determined by errors of the parameters of the regression line best fitted into the experimental data associated with Se extrapolating the flat part between the Se and Cu surface peaks. An error of the normalised Cu minimum yield of ±19.0% is very significant. It also includes both the error of extrapolating the regression lines up to the channels corresponding to Y_{minSe} in the Se aligned yield and the error of Y_{RSe} in the Se random yield extrapolated by $A/(E_0+E)^2$ at the corresponding channels. Because it exceeds the normalised minimum yield of Cu we can estimate only the upper possible limit of χ_{minCu} to be about 25%. However the precision, calculated from the scatter of χ_{minCu} in the three aligned spectra is very reasonable ±0.8% and shown in Table 1.

The normalised minimum yield χ_{min} in a monatomic lattice can be expressed [16] as:

$$\chi_{min} = \pi N d r_{min}^2, \tag{3}$$

where r_{min} is the closest distance of approach between the channeling ion and the row of atoms along the axis of channeling and N atomic concentration. The ions approaching closer than r_{min} dechannel. The most accurate reported theoretical value of χ_{min} can be determined from an empirical function best fitted into computer calculated energy dependence of minimum yield [19]:

$$\chi_{min-th} = 18.8 N d u^2 \sqrt{1 + [126u/(\psi_{1/2} d)]^{-2}}, \tag{4}$$

where u is the mean square amplitude of thermal vibrations of the atoms, constituting the axis of channeling, in the plane perpendicular to this axis. These amplitudes, derived by Zahn and Paufler [20] for Cu, In, and Se atoms in the $CuInSe_2$ lattice from the Debye–Waller temperature factors assuming isotropic distribution, are shown in Table 1.

Theoretical estimates of the normalised minimum yields $\chi_{min\text{-}th}$, were calculated using expression (4) for each of the $CuInSe_2$ sublattices assuming u and N values for Cu, In and Se. These $\chi_{min\text{-}th}$ are shown in Table 1. A comparison of $\chi_{min\text{-}th}$ and $\chi_{min\text{-}ex}$ demonstrates that the theoretical values are smaller than the experimental ones although being in the close range. Similar discrepancies have been reported for other material with monatomic lattices as well as compounds [17] and attributed to surface contamination as well as to the presence of structural defects in the lattices.

The surfaces of the analysed samples were prepared using the standard procedure [10] suggesting that the differences between $\chi_{min\text{-}th}$ and $\chi_{min\text{-}ex}$ can rather be related to differences in the volume concentrations of defects. Normalised defect concentration n_d can be estimated [21] using the following expression:

$$n_d = \frac{N_d}{N} = \frac{\chi_{min-ex} - \chi_{min-th}}{1 - \chi_{min-th}}, \tag{5}$$

where N_d is the concentration of atoms displaced from their lattice sites into interstitial positions, where they block the channels, causing an increase of backscattering which was not taken in account in expression (4) and n_d is the fraction of the displaced atoms. Such fractions of copper, indium and selenium scattering centres were calculated at the assumption of a homogeneous distribution of the channeling ion flux in the transverse plane of the channels and randomly distributed scattering centres. For more accurate calculations of the concentrations of displaced atom dechanneling cross-sections depending on the defect nature and their lattice locations as well as flux peaking of channeling ions should be taken into account. Without such additional information the determined values of n_d can be used as first order estimates of the fraction of the lattice atoms shifted from the lattice sites to interstitial positions. The absolute accuracy of such estimates can be particularly low, in the case of extended defects which have rather different dechanneling effects in comparison with arrays of randomly distributed interstitial atoms. But for relative comparisons of the defect concentration the method can give interesting and unique information.

The values of n_d, calculated for the Cu, In and Se sublattices using $\chi_{min\text{-}th}$ and $\chi_{min\text{-}ex}$, are shown in Table 1. The estimated upper limit of the defect concentration in each of the Se and Cu sublattices can be up to 2.5×10^{21} cm^{-3} due to the uncertainties of calculations of the normalised minimum yields. The absolute concentrations of defects for each of the three sublattices are also shown in Table 1. The total concentration of defects as the sum of that in each sublattice is 1.2×10^{21} cm^{-3} whereas its upper limit can be as high as 12% of all atoms. The errors of these estimates, shown in Table 1, are precision for the three aligned spectra and do not reflect the accuracy of the dechanneling model.

4. Discussion

The defect concentrations shown in Table 1 are significantly higher than that of the donors and acceptors obtained from Hall measurements [3,4], optical absorption [5] or DLTS [6]. This discrepancy can be explained by differences in the scope of defects each particular technique is sensitive to. For example a high level of compensation in the material, which contains nearly equal concentrations of donors and acceptors leaving net concentrations of the charge carriers of $10^{16} - 10^{17}$ cm^{-3}. However the total defect concentration of 7×10^{20} cm^{-2}, determined using neutron scattering [7], in $CuInSe_2$ with similar copper to indium ratios is quite close to our estimate of 1.2×10^{21} cm^{-3}. A similar value of 8.5×10^{20} cm^{-2} has been determined by Neumann [13] for a $CuInSe_2$ single crystals with $\chi_{min} = 6\%$. Analysing χ_{min} only in the indium sublattice and then assigning the obtained defect concentration to the whole lattice resulted in an underestimation of final values.

Comparing the fractions of displaced atoms in different sublattices in Table 1 one can see that n_d in the Se and especially in the Cu sublattices are significantly greater than that in the In one suggesting that the fractions of Cu and Se atoms displaced from their lattice sites to interstitial positions are greater than that of In.

Such interstitial positions could be copper and selenium interstitial atoms, Cu_i and Se_i, respectively. The transverse plane distribution of the channeling ions in the near surface layer is essentially inhomogeneous due to the flux peaking effect [22]. The concentration of channeling ions at the channel centre is significantly higher than that close to strings of atoms. Considering the presence of Cu_i and Se_i we can expect their concentrations to be significantly smaller than the values in Table 1. The monovalent nature of copper leads to a low formation energy of copper vacancies [23] and high mobility of interstitial copper atoms [24] making these defects quite likely to be present in $CuInSe_2$.

On the other hand the high χ_{Amin} for the Se sublattice is quite consistent with the presence of high concentrations of copper vacancies V_{Cu}. Every copper atom in the $CuInSe_2$ lattice bonds four selenium atoms. The presence of a copper vacancy should induce small shifts of four Se atoms surrounding such a vacancy. A low formation energy of V_{Cu} is predicted by theoretical studies [23]. The presence of V_{Cu} is supported by the direct observation of such vacancies in $CuInSe_2$ single crystals using scanning tunnelling microscopy (STM) [25]. Also the STM studies demonstrated the presence of indium on copper site In_{Cu}. Such defect as well as copper on indium site Cu_{In} should also generate small shifts of the surrounding selenium atoms from their lattice positions. Recent neutron diffraction experiments on $CuInSe_2$ with the similar copper to indium ratios [7] also suggest the presence of V_{Cu} and Cu_{In} at concentrations of 4×10^{20} and 3×10^{20} cm^{-3}.

Thus the presence of high concentrations of copper vacancies, antisite defects In_{Cu} and Cu_{In}, as well as relatively small concentrations of Cu_i can explain high dechanneling rates in high structural quality $CuInSe_2$ single crystals.

5. Conclusions

Single crystals of $CuInSe_2$ have been studied by the Rutherford backscattering of 2 MeV helium ions involving axial channeling along the $\langle 221 \rangle$ direction. Experimentally determined critical angle $\psi_{1/2}$ and normalised minimum yield χ_{min} were compared with theoretical values. The concentration of point defects in the Cu, In, and Se sublattices, derived from χ_{min}, was estimated to be 4.9×10^{20}, 1.0×10^{20} and 5.7×10^{20} cm^{-3}, respectively.

Acknowledgements

This work has been supported by RFBR grants 10-03-96047 and 11-03-00063.

References

[1] P. Jackson, D. Hariskos, E. Lotter, S. Paetel, R. Wuerz, R. Menner, W. Wischmann, M. Powalla, Prog. Photovoltaics Res. Appl. 19 (2011) 894.
[2] W. Shockley, H.J. Queisser, J. Appl. Phys. 32 (1961) 51.
[3] H. Neumann, R.D. Tomlinson, Solar Cells 28 (1990) 301.
[4] C. Rincon, C. Bellabara, Phys. Rev. B: Condens. Matter 33 (1986) 7160.
[5] I. Dirnstorfer, M. Wagner, D.M. Hofmann, M.D. Lampert, F.B. Karg, B.K. Meyer, Phys. Status Solidi A 168 (1998) 163.
[6] A.L. Li, J. Shih, J. Electron. Mater. 22 (1993) 195.
[7] C. Stephan, S. Schorr, M. Tovar, H. Schock, Appl. Phys. Lett. 98 (2011) 091906.
[8] E. Korhonen, K. Kuitunen, F. Tuomisto, A. Urbaniak, M. Igalson, J. Larsen, L. Gütay, S. Siebentritt, Y. Tomm, Phys. Rev. B: Condens. Matter 86 (2012) 064102.
[9] W.K. Chu, J.W. Mayer, M.A. Nicolet, Backscattering Spectrometry, Academic Press, New York, San Francisco, London, 1978.
[10] M.V. Yakushev, G. Lippold, A.E. Hill, R.D. Pilkington, R.D. Tomlinson, J. Mater. Sci. –Mater. Electron. 7 (1996) 155.
[11] M. Yakushev, A. Zegadi, H. Neumann, P.A. Jones, A.E. Hill, R.D. Pilkington, M.A. Slifkin, R.D. Tomlinson, Cryst. Res. Technol. 29 (1994) 427.
[12] M.V. Yakushev, I.I. Ogorodnikov, V.A. Volkov, A.V. Mudryi, J. Vac. Sci. Technol., A 29 (2011) 051201.
[13] H. Neumann, Cryst. Res. Technol. 29 (1994) 985.
[14] R.D. Tomlinson, Solar Cells 16 (1986) 17.
[15] J.L. Shay, J.H. Wernick, Ternary Chalcopyrite Semiconductors-Growth, Electronic Properties, and Applications, Pergamon, New York, 1975.
[16] J. Lindhard, Mat. Fys. Medd. Dan. Vid. Selsk. 34 (1965) 14.
[17] S.T. Picraux, J.A. Davies, L. Eriksson, N.G.E. Johansson, J.W. Mayer, Phys. Rev. 180 (1969) 873.
[18] G. Bohm, G. Zech, Introduction to Statistics and Data Analysis for Physicists, Verlag Deutsches Elektronen-Synchrotron (2010). http://www-library.desy.de/l-books.html.
[19] L.C. Feldman, J.W. Mayer, Fundamentals of Surface and Thin Film Analysis, North-Holland, New York, 1986.
[20] G. Zahn, P. Paufler, Cryst. Res. Technol. 23 (1988) 499.
[21] E. Bogh, Can. J. Phys. 46 (1968) 653.
[22] D.V. Morgan, D. Van Vliet, Radiat. Effects 12 (1972) 203.
[23] S.B. Zhang, S.-H. Wei, A. Zunger, H. Katayama-Yosida, Phys. Rev. B: Condens. Matter 57 (1998) 9642.
[24] V. Nadazdy, M. Yakushev, E.D. Djebbar, A.E. Hill, R.D. Tomlinson, J. Appl. Phys. 84 (1998) 4322.
[25] L. Kazmerski, Vacuum 43 (1992) 101.